Design of DGS Compact UWB Antenna for C-, X-, Ku-, and Ka-Band Applications Using ANN and ANFIS Optimization Techniques

Rakesh K. Maurya, Binod Kumar Kannaujia, Ajay K. Maurya, and Ravi Prakash

Abstract A novel tapered and slot loaded compact circular microstrip patch antenna (TSCCMPA) with DGS for ultra-wideband (UWB) applications is proposed. For designing of UWB TSCCMPA, a move toward optimizing the physical stricture, two vigorous techniques, namely, artificial neural network (ANN) and adaptive neuro-fuzzy inference system (ANFIS) are used. Commercially available Ansoft HFSS v.13 is utilized to extract the 144 datasets of TSCCMPAs having different sensitive parameters related to antenna dimensions and substrate materials. Apart from 144 simulated datasets, 129 were used for training and remaining 15 were utilized for testing of models. The average percentage errors (APE) for resonant frequencies of return loss are calculated regarding performance of tested datasets of ANN and ANFIS model. The APE in ANN and ANFIS model found in testing of resonant frequencies f_1 and f_2 are 0.8731%, 0.0699%, and 0.7698%, 0.0607%, respectively. The very low APE indicates that the models can be successfully applied for optimization of physical parameter of UWB TSCCMPA for computer-aided design (CAD) applications. The trained models can be used effectively for antenna parameter estimation, instead of running HFSS repetitively or other optimization techniques, which consume more time. Successful implementation of TSCCMPA shows broader impedance bandwidth of 2.6–53.5 GHz as 180% at 26.00 GHz of center frequency. The average gain of proposed antenna is found as 4.14 dBi. Due to very wideband the anticipated antenna can be effectively used in many applications.

Keywords Compact UWB microstrip antenna · Tapered and slotted circular microstrip patch · Artificial neural network · Adaptive neuro-fuzzy interface system · Computer-aided design

R. K. Maurya (✉)
Department of Electronics and Instrumentation Engineering, Faculty of Engineering and Technology, MJP Rohilkhand University, Bareilly, U.P. 243006, India
e-mail: rakesh_maurya@mjpru.ac.in

B. K. Kannaujia
School of Computation and Integrative Sciences, JNU, New Delhi 110067, India

A. K. Maurya · R. Prakash
Departmet of Electronics Engineering, UNS, IET, VVS Purvanchal University, Jaunpur, India

S. Rawat et al. (eds.), *Proceedings of First International Conference on Computational Electronics for Wireless Communications*, Lecture Notes in Networks and Systems 329,
https://doi.org/10.1007/978-981-16-6246-1_1

1 Introduction

Need of miniaturization and bandwidth enhancement of microstrip patch antenna (MPA) is today's challenge of researcher's due to portability and uniqueness features of MPA which covers maximum bands of communication applications. In this stare, many researchers used substrate material with high dielectric constant in traditional MPA, and have achieved miniaturization but the bandwidth and efficiency decreased [1–3]. Most of them have tried to overcome this problem by applying slit/slot loading in MPAs [4–9], sorting pins [10–12], sorting walls [13], and slot loaded patch [14–16] in traditional MPA and somehow succeeded to reduce the size but not even more for bandwidth enhancement. For bandwidth enhancement, the DGS MPA has been recently investigated [17–20] and the bandwidth enhancement up to 90% has been achieved.

To achieve compactness and bandwidth enhancement in the designing of traditional MPA, the analysis techniques such as cavity model [21] and transmission line model [22] were implemented. But the complicated shapes of MPA can't be analyzed with these traditional techniques. Hence, some other powerful techniques such as method of moment [23] and finite difference time domain method [24] are used. But again these techniques involve rigorous mathematical formulation with extensive numerical procedure, hence more time-consuming. In many of previous efforts, some of them tried to intend UWB MPA by these parametric analyses, and they have altered the parameters accordingly and achieved UWB characteristics [25–29]. Nowadays, most powerful software such as IE3D, HFSS, and CST Studio are widely used for analysis of any type of antenna and other microwave structure with trial-and-error basis [5, 10, 17–20]. Hence, again more time-consuming and has no guaranteed to attain an enviable goal even after numerous trial.

Recently, ANN, ANFIS, support vector machine (SVM), etc. techniques have been used efficiently for analysis of any types of MPA without any rigorous calculation and time consumption. Because once a model of ANN, ANFIS, and/or SVM has been designed for a MPA then it can be used many times at no time cost. Most of the researchers [30–37] have successfully used the ANN, ANFIS, and SVM to analyze the various parameters of MPAs and design the model.

In this paper, a novel tapered and slot loaded compact circular MPA with dimension of 20×20 mm^2, significantly smaller than the antenna reported in above discussion, is proposed for UWB application like C, X, Ku, Ka, etc. The proposed work is followed by parametric analysis with the help of ANN and ANFIS model. The basic design procedure of ANN and ANFIS model for proposed MPA is shown in Fig. 1. ANN and ANFIS model is designed to compute the accurate resonant frequencies of proposed UWB TSCCMPA.

To design the ANN and ANFIS model, 144 datasets were collected with the help of commercially available Ansoft HFSS v.13. Apart from 144 simulated datasets, 129 were used for training the models and remaining 15 were utilized for testing the accuracy of models.

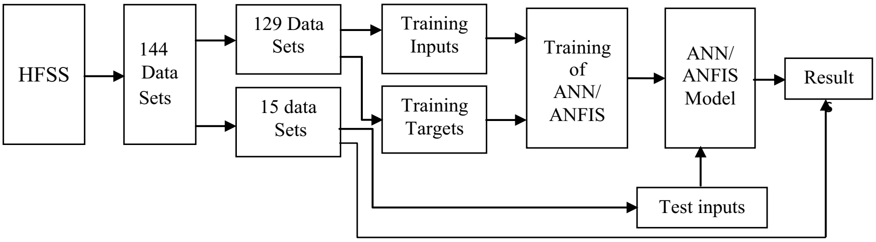

Fig. 1 Basic design procedure of ANN and ANFIS model of proposed UWB TSCCMPA

The proposed work is divided mainly into three parts (i) antenna structure and collection of input output datasets by using HFSS v.13, (ii) design of ANN and ANFIS model for computing resonant frequencies using simulated datasets, and (iii) results and discussion.

2 Antenna Structure and Simulation

Figure 2 exhibits the geometry of compact ($W = 20$ mm, $L = 20$ mm) UWB microstrip feed TSCCMPA. The MPA consists of a circular patch of radius r tapered with angle

Fig. 2 Geometry of proposed UWB TSCCMPA

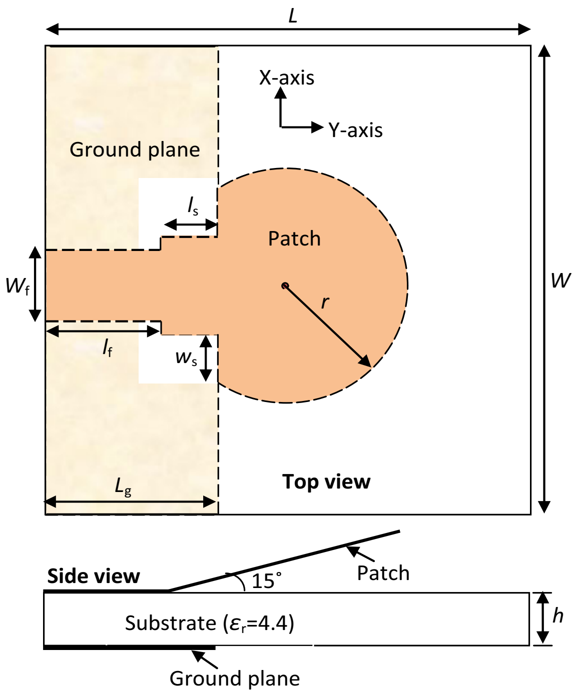

Table 1 Physical and electrical parametric sets of 144 simulated UWB TSCCMPAs

Number of simulation sets	Physical and electrical parameters					
	r (mm)	l_s (mm)	w_s (mm)	ϕ (degree)	h (mm)	ε_r
36	4.5	1.5 1.8	1.3 1.6	10, 15, 20	0.8, 1.6	2.2, 2.33, 4.4
36	5.0	1.8 2.0	2.0 2.0	15, 20, 25	0.8, 2.5	2.33, 4.4, 6.15
36	5.5	2.1 2.4	1.9 2.2	10, 15, 25	1.6, 3.2	2.2, 4.4, 6.15
36	6.0	2.4 2.7	2.2 2.5	20, 25, 30	3.2, 2.5	2.33, 4.4, 6.15

ϕ with two symmetrical slot of $w_s \times l_s$ at feed side, engraved into a dielectric substrate (20 mm × 20 mm) of thickness h, loss tangent of tan δ, and relative permittivity of ε_r. An open-ended microstrip line (50-Ω) feed of width $w_f \times l_f$ is placed on opposite side of the ground plane. The ground is defected, i.e., reduced rectangular size of 6 mm × 20 mm is taken at the opposite of feed as shown in Fig. 2. In proposed MPA, we have applied three techniques to achieve UWB antenna, i.e., two symmetrical slots on circular patch, tapering the patch and a partial ground plane.

In order to conclude the values of f_1 and f_2 of UWB for ANN and ANFIS model, the simulation is performed by HFSS v.13. The 144 TSCCMPAs having various sets of sensitive parameters of antenna proportions and substrate material are listed in Table 1. These sets of UWB TSCCMPA operate in band width of 2.3–53.5 to 3.4–54.6 GHz corresponding in C-, X-, Ku-, and Ka-bands. The 129 randomly selected input–output datasets of UWB TSCCMPA were used for training the ANN and ANFIS for designing the model, and rest 15 were utilized to test the accuracy of model.

3 Design of ANN and ANFIS Models

3.1 Design Procedure of ANN Model

ANN is one of the most intelligent, fast, and flexible tools to model nonlinear relation, simulation, and optimization of antenna [38]. The ANN, CAD models are very much popular nowadays, due to accuracy in results, learning ability and adaptability, very less information obligation, fast real-time retort, and easy execution attribute. For better model of a particular problem, many of basic parameters of ANN are settled on trial-and-error basis. Once an accurate model is ready then it can be used number of times without any time cost. The basic parameters of ANN are: network architecture, hidden layers, neurons in hidden layer, learning algorithm, activation functions, etc. Two special classes of ANN architecture, Multi-layer Perceptrons (MLPs) [39] and Radial-basis Function Networks (RBFNs) [40] have been widely used to analyze this type of problem. In this paper, MLP network architecture is used. MLP has three types of layers: input layer, output layer, and one or more hidden layers. Results of MLPs for a meticulous problem depend on using suitable learning algorithm. After several trials for proposed work, the Levenberg–Marquardt (LM) algorithm is found suitable. The accurate ANN synthesis model needed a suitable number of neurons in hidden layers. For proper configuration of hidden layers of proposed model, many trials were carried out by changing the epoch, neurons, and activation functions in layers. High precision is achieved using MLP with two hidden layer networks. Finally, the ANN model has total four layers (two hidden layers, one input layer, and one output layer). Finally, the appropriate network configuration was found $6 \times 28 \times 12 \times 2$, which means that number of neurons are 6, 28, 12, and 2 in input layer, first, second hidden layers, and output layer, respectively. The activation function which is found suitable in both input and output layers was linear and tangent sigmoid activation function is found suitable for hidden layers. Initial weights of ANN model are set up arbitrarily. The weights adoption used mean square error (MSE) between target and output of ANN. The training epoch was found 543 for accurate model. Finally, the ANN model for proposed UWB TSCCMPA is shown in Fig. 3.

The accurateness of ANN-based analysis model depends on datasets used during training. Collections of more sets of data give more accurate result. The training and test datasets were generated from HFSS v.13 shown in previous section. Now the collected datasets were arranged in six-row input matrix (r, l_s, w_s, ϕ, h, and ε_r) and two-row target matrix (f_1 and f_2). Before training, the datasets were scaled in $[-1, +1]$ to each row of input as well as output matrix for easier learning process. Training process curtails the training error between ANN output and target output. The training error is checked by mean square error (MSE) performance graph. In

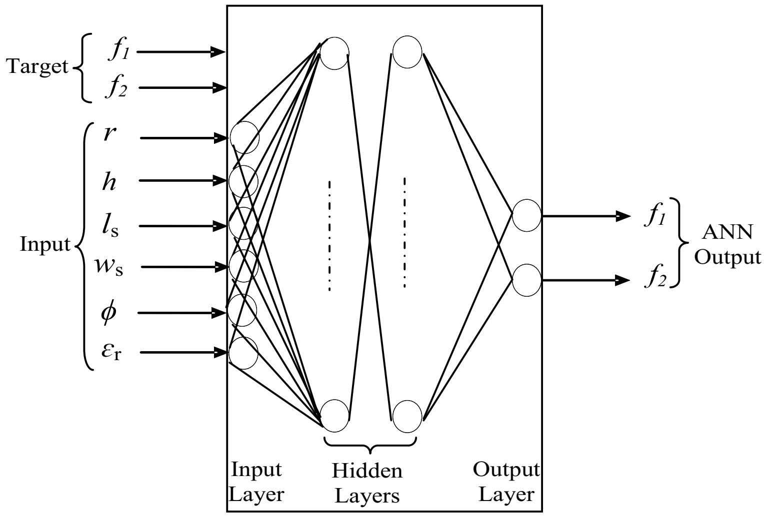

Fig. 3 ANN model of proposed UWB TSCCMPA

Table 2 The comparative results of HFSS (simulation), ANN, and ANFIS of proposed UWB TSCCMPA

Test patches	Input dimensions (mm)						Results (GHz)					
	r	l_s	w_s	Φ	h	ε_r	HFSS		ANN		ANFIS	
							f_1	f_2	f_1	f_2	f_1	f_2
1	4.5	1.5	1.3	15	0.8	4.4	4.582	46.552	4.540	46.577	4.555	46.578
2	4.5	1.8	1.6	10	0.8	2.33	4.625	46.992	4.657	46.967	4.651	46.971
3	4.5	1.8	1.6	20	1.6	2.2	5.071	47.417	5.112	47.389	5.109	47.392
4	5.0	1.8	2.0	15	0.8	2.33	4.937	46.148	4.965	46.179	4.961	46.175
5	5.0	2.0	2.0	15	0.8	4.4	4.900	46.660	4.677	46.598	4.674	46.591
6	5.0	1.8	2.0	20	2.5	2.33	6.884	48.588	6.851	48.551	6.855	48.557
7	5.0	2.0	2.0	20	0.8	6.15	6.422	48.225	6.449	48.258	6.446	48.252
8	5.0	2.0	2.0	25	2.5	6.15	5.871	47.844	5.845	47.877	5.850	47.869
9	5.5	2.1	1.9	10	1.6	4.4	6.461	48.692	6.497	48.728	6.490	48.722
10	5.5	2.1	1.9	25	3.2	2.2	5.818	47.567	5.839	47.592	5.836	47.588
11	5.5	2.4	2.2	15	1.6	6.15	3.229	45.094	3.253	45.125	3.251	45.119
12	5.5	2.4	2.2	15	3.2	2.2	3.466	45.347	3.497	45.312	3.492	45.323
13	6.0	2.4	2.2	20	2.5	4.4	4.893	47.495	4.862	47.471	4.873	47.473
14	6.0	2.7	2.5	30	2.5	4.4	6.056	48.884	6.089	48.850	6.081	48.857
15	6.0	2.7	2.5	25	3.2	6.15	5.990	47.503	5.961	47.539	5.967	47.533
Average Percentage Error (APE)									0.8731	0.0699	0.7698	0.0607

the training, when MSE is found near to zero, then training process stopped and the model is ready. The trained model is then validated by test inputs of 15 remaining input datasets, which is already extracted by HFSS v.13. Then APE of test output of model is calculated and shown in Table 2. The formula for the calculation of APE [30] is

$$\text{APE} = \frac{\sum \left| \left(f_{\text{FHSS}} - f_{\text{ANN/ANFIS}} \right) / f_{\text{HFSS}} \right|}{\text{number of antenna}} \times 100 \quad (1)$$

3.2 Design Procedure of ANFIS Model

ANFIS is a universal estimator [41], it combines the benefits of ANN and fuzzy inference system (FIS) in a single sculpt. FIS is an estimating tool, which is based on fuzzy set theory, fuzzy if then rules, and fuzzy reckoning. The neuro-adaptive learning methods for the membership function (MF) parameters of fuzzy system are similar to those used in neural network training. Hence, ANFIS is FIS execution in the scaffold of an adaptive fuzzy neural network, which is a very influential approach

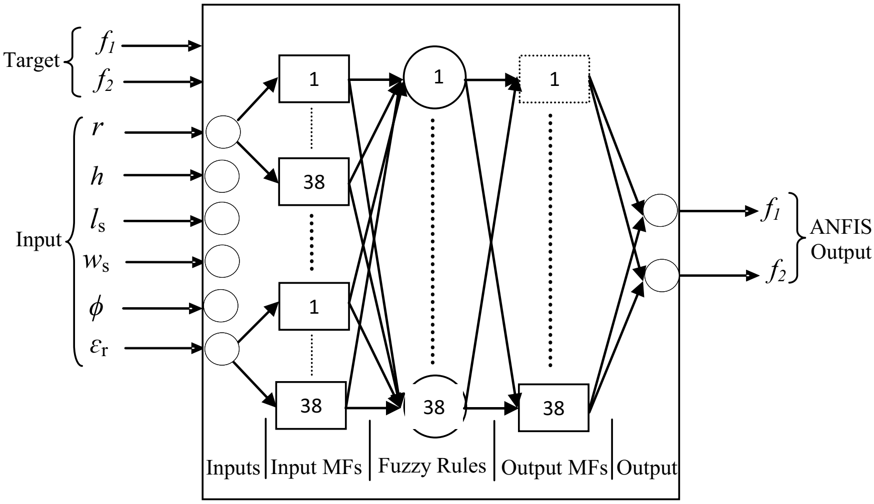

Fig. 4 ANFIS model of proposed UWB TSCCMPA

for analyzing nonlinear and complex association of input and output sets of data. The ANFIS architecture of proposed MPA is shown in Fig.4, which consists of five steps: inputs, membership functions of input, fuzzy rules, membership functions of output, and outputs.

For the best model for a particular problem, many of basic parameters of ANFIS are settled on trial-and-error basis. Once an accurate model is ready, then it can be used number of times without any time cost. After many trials in training of 129 input–output datasets (same datasets used in training of ANN), the following parameter of ANFIS model is found suitable for proposed MPA. These suitable ANFIS parameters are ANFIS model type-Sugeno, input/output MF type- Gaussian/linear, number of MFs-38, number of fuzzy rules-38, and training epochs-122. Again as in ANN, after designing the model remaining 15 input sets of data were used for testing of the model. Then APE of tested output of 15 datasets of ANFIS model is calculated and shown in Table 2.

4 Result and Discussion

The return loss characteristics, radiation pattern, and antenna gain of proposed UWB TSCCMPA are shown in Figs. 5, 6, and 7, respectively. In Fig. 5, it can be seen as a UWB performance of 51 GHz (2.6–53.5 GHz) impedance BW below 10 dB of return loss. Figure 6a and b shows the radiation pattern at resonant frequencies f_1 and f_2 for the proposed UWB TSCCMPA. The radiation patterns are almost stable across the entire operating frequency band. Variation of gain (dBi) w.r.t. frequency

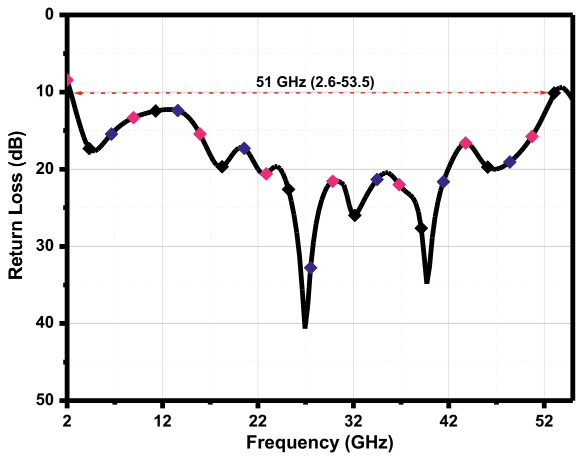

Fig. 5 Simulated return loss of proposed UWB TSCCMPA

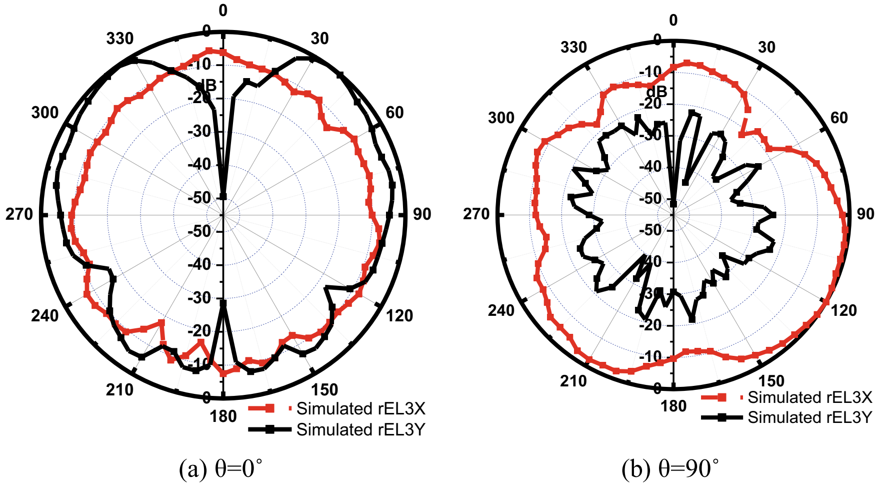

Fig. 6 Simulated radiation pattern for center frequency ($f_1 = 27$ GHz) of proposed UWB TSCCMPA

of the proposed antenna is shown in Fig. 7. The average gain of proposed antenna is found as 4.14 dBi.

The optimized ANN and ANFIS model has been fruitfully introduced for the analysis of UWB TSCCMPA. The HFSS simulation results and ANN, ANFIS tested results are shown in Table 2. These results are in very good agreement, which agreed the validity of ANN and ANFIS model. The results shown in Table 2 are enough to verify the proposed ANN and ANFIS model. The better results may be obtained

Fig. 7 Simulated gain of proposed UWB TSCCMPA

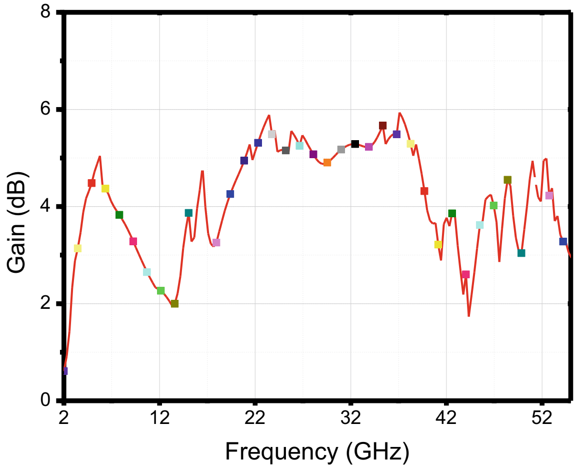

by wishing other training and test datasets from the ones used in this paper, or by collecting more dataset values for training and testing.

References

1. R. Garg, P. Bhartia, I. Bahl, A. Ittipihoon, *Microstrip Antenna Design Handbook* (Artech House, London, 2001)
2. N. Kumar, P. Kumar, M. Sharma, Reconfigurable antenna and performance optimization approach. Wireless Pers. Commun. **112**, 2187–2212 (2020). https://doi.org/10.1007/s11277-020-07145-0
3. G. Kumar, K.P. Ray, *Broadband Microstrip Antennas* (Artech House, USA, 2003)
4. A.A. Deshmukh, G. Kumar, Formulation of resonant frequency for compact rectangular microstrip antennas. Microw. Opt. Technol. Lett. **49**(2), 498–502 (2007)
5. A.K. Gautam, B.K. Kanaujia, A novel dual band asymmetric slit with defected ground structure for circular polarization operation. Microw. Opt. Technol. Lett. **55**, 1198–1202 (2013)
6. B.L. Ooi, Q. Shen, A novel E-shaped broadband microstrip patch antenna. Microw. Opt. Technol. Lett. **27**(5), 348–353 (2000)
7. A.F. Sheta, A. Mohra, S.F. Mahmoud, Multi-band operation of a compact H-shaped microstrip antenna. Microw. Opt. Technol. Lett. **35**, 363–368 (1982)
8. W. Chew, A broad-band annular-ring microstrip antenna. IEEE Trans. Antennas Propag. **30**(5), 918–923 (1982)
9. K.L. Wong, S.C. Pan, Compact triangular microstrip antenna. Electron. Lett. **33**, 433–435 (1997)
10. M.K. Khandelwal, B.K. Kanaujia, S. Dwari, S. Kumar, A.K. Gautam, Analysis and design of wide band microstrip-line-fed antenna with defected ground structure for Ku band application. Int. J. Electron. Commun. (AEU) **68**, 951–958 (2014)
11. N.P. Gupta, M. Kumar, Development of a reconfigurable and miniaturized CPW antenna for selective and wideband communication. Wireless Pers. Commun. **95**, 2599–2608 (2017). https://doi.org/10.1007/s11277-017-3942-8
12. S.C. Pan, K.L. Wong, Dual-frequency triangular microstrip antenna with a shorting pin. IEEE Trans. Antennas Propagat. **45**, 1889–1892 (1997)

13. Y.X. Guo, K.M. Luk, K.F. Lee, L-probe proximity-fed short-circuited patch antenna. Electron. Lett. **35**, 2069–2071 (1999)
14. K.L. Wong, K.P. Yang, Compact dual-frequency microstrip antenna with a pair of bent slots. Electron. Lett. **34**, 225–227 (1998)
15. W.S. Chen, C.K. Wu, K.L. Wong, Compact circularly polarized microstrip antenna with bent slots. Electron. Lett. **34**, 1278–1280 (1998)
16. S. Saxena, B.K. Kanaujia, S. Dwari, S. Kumar, R. Tiwari, A Compact microstrip fed dual polarized multiband antenna for IEEE 802.11 a/b/g/n/ac/ax applications. Int. J. Electron. Commun. (AEU) **72**, 95–103 (2017)
17. A.K. Gautam, S. Yadav, B.K. Kanaujia, A CPW-Fed compact UWB Microstrip antenna. IEEE Antenna Wireless Propag. Lett. **12**, 151–157 (2013)
18. K.H. Chiang, K.W. Tam, Microstrip monopole antenna with enhanced bandwidth using defected ground structure. IEEE Antennas Wireless Propag. Lett. **7**, 532–536 (2008)
19. R.K. Maurya, B.K. Kanaujia, A.K. Gautam, S. Chatterji, A.K. Singh, Circularly polarized hexagonal ring microstrip patch antenna with asymmetrical feed and DGS. Microwave Opt. Technol. Lett. 1–7 (2019)
20. N. Kishore, A. Prakash, V.S. Tripathi, A reconfigurable ultra-wide with defected ground structure for ITS application. Int. J. Electron. Commun. (AEU) **72**, 210–216 (2017)
21. W.F. Richards, Y.T. Lo, D.D. Hirrisson, An improved theory for microstrip antenna application. IEEE Trans. Antennas Propag. **29**, 84–87 (1981)
22. K. Bhattacharya, R. Garg, A generalized transmission line model for microstrip patches. IEE Proc. Microwave Antenna Propag. **132**, 93–99 (1985)
23. R.F. Harrington, *Field Computation by Moment Method* (IEEE Press, Piscataway NJ, 1993)
24. A. Taflove, *Computational Electrodynamics. The Finite Difference Time Domain* (Artech House, Baston, 1995)
25. J.X. Liang, C.C. Chiau, X.D. Chen, C.G. Parini, Study of a printed circular disc monopole antenna for UWB systems. IEEE Trans. Antennas Propag. **53**(11), 3500–3505 (2005)
26. M. John, M.J. Ammann, Optimization of impedance bandwidth for the printed rectangular monopole antenna. Microw. Opt. Technol. Lett. **47**(2), 153–155 (2005)
27. A.A. Eldek, Numerical analyses of a small ultra wideband microstrip-fed tap monopole antenna. Progress Electromagn. Res. **65**, 59–69 (2006)
28. R. Fallahi, A.A. Kalteh, M.G. Roozbahani, A novel UWB elliptical slot antenna with band-notched characteristics. Progress Electromagn. Res. **82**, 127–137 (2008)
29. M. Sadat, M. Houshmand, M. Roshandel, Design of a microstrip square-ring slot antenna filled by an H-shaped slot for UWB applications. Progress Electromagn. Res. **70**, 191–199 (2007)
30. A. Akdagli, A. Toktas, A. Kayabasi, I. Develi, An application of artificial neural network to compute the resonant frequency of E-shaped compact microstrip antennas. J. Electr. Eng. Elektrotechnicky Casopis **64**(5), 317–323 (2013)
31. T. Khan, A. De, A generalized ANN model for analyzing and synthesizing rectangular, circular, and triangular microstrip antennas. Hindawi Publishing Corp. Chin. J. Eng. **647191**, 1–9 (2013)
32. U. Chourasia, S. Silakari, Adaptive neuro fuzzy interference and PNN memory based grey wolf optimization algorithm for optimal load balancing. Wireless Pers. Commun. (2021). https://doi.org/10.1007/s11277-021-08400-8
33. R.K. Maurya, M.S. Vijay, N. Chaudhary, D. Kumar, Model for calculation of patch radius of circular microstrip antenna using artificial neural network. IEEE Int. Conf. **39**, 167–174 (2013). https://doi.org/10.1109/ICMIRA
34. H.J. Song, C.Y. Miao, Z.Q. Shen, W. Roel, D.H. Maja, C. Francky, Design of fuzzy cognitive maps using neural networks for predicting chaotic time series. Neural Netw. **23**(10), 264–275 (2010)
35. Z.B. Wang, S.J. Fang, Q. Wang, H.M. Liu, An ANN based synthesis model for the single-feed circularly-polarized square microstrip antenna with truncated corners. IEEE Trans. Antennas Propag. **60**, 5989–5993 (2012)
36. T.W.L. Wang, C. Quek, P. Cheng, GenSo-EWS: a novel neural-fuzzy based early warning system for predicting bank failures. Neural Netw. AEU **17**(4), 567–587 (2004)

37. A. Kayabasi, A. Akdagli, Predicting the resonant frequency of E-shaped compact microstrip antennas by using ANFIS and SVM. Wireless Pers. Commun. **82**, 1893–1906 (2015)
38. Q.J. Zhang, K.C. Gupta, *Neural Network for RF and Microwave Design* (Artech House: Norwood, Mass, USA, 2000)
39. E.D. Ubeyli, I. Guler, Multilayer perceptron neural network to compute quasistatic parameter of asymmetric coplanar waveguides. Neurocomputing **62**, 349–365 (2004)
40. R.K. Mishra, A. Patnaik, Neural network based CAD model for the design of square patch antennas. IEEE Trans. Antenna Propag. **46**, 1890–1892 (1998)
41. J.S.R. Jang, C.T. Sun, E. Mizutani, *Neuro-Fuzzy and Soft Computing* (Prentice Hall, 1997), pp. 335–368